



## Low mass stellar companions around four giant stars



M. Yılmaz<sup>a,e,\*</sup>, I. Bikmaev<sup>b,d</sup>, B. Sato<sup>c</sup>, S.O. Selam<sup>a</sup>, A.I. Galeev<sup>b,d</sup>, V. Keskin<sup>e</sup>, H. Izumiura<sup>f</sup>, E.N. Irtuganov<sup>b,d</sup>, E. Kambe<sup>f</sup>, İ. Özavcı<sup>a</sup>, S.S. Melnikov<sup>b,d</sup>, R.Ya. Zhuchkov<sup>b,d</sup>, N. Okada<sup>g</sup>

<sup>a</sup>Ankara University, Faculty of Science, Department of Astronomy and Space Sciences, TR-06100 Tandoğan, Ankara, Turkey

<sup>b</sup>Department of Astronomy and Satellite Geodesy, Kazan Federal University (KFU), 420008 Kazan, Russia

<sup>c</sup>Tokyo Institute of Technology, 2-12-1 Ookayama, Meguro-ku, Tokyo 152-8550, Japan

<sup>d</sup>Academy of Sciences of Tatarstan, Bauman Str, 20, 420111 Kazan, Russia

<sup>e</sup>Ege University, Faculty of Science, Department of Astronomy and Space Sciences, TR-35100 Bornova, İzmir, Turkey

<sup>f</sup>Okayama Astrophysical Observatory, National Astronomical Observatory, Honjo 3037-5, Kamogata, Okayama 719-0232, Japan

<sup>g</sup>Advanced Technology Center, National Astronomical Observatory, Osawa 2-21-1, Mitaka, Tokyo 181-8588, Japan

### HIGHLIGHTS

- Three low-mass mass companions found around four intermediate-mass giants.
- The stellar parameters of HD1695, HD120235, HD145316 and HD200004 were derived.
- The orbital parameters of the companions are also derived.
- The most significant result is related HD120235, which have a highly eccentricity.
- The eccentricity value is the largest one known for a SB1.

### ARTICLE INFO

#### Article history:

Received 21 February 2014

Received in revised form 4 June 2014

Accepted 5 June 2014

Available online 17 June 2014

Communicated by W. Soon

#### Keywords:

Stars: individual

Stars: abundances

Techniques: radial velocities

Miscellaneous: binary

### ABSTRACT

We present three low-mass and one solar mass companions found around four intermediate-mass giants HD1695, HD120235, HD145316 and HD200004 from precise radial velocity measurements using the 1.5 m Russian-Turkish Telescope (RTT150) at the TÜBİTAK National Observatory of Turkey (TUG). The stellar parameters, which are effective temperature ( $T_{\text{eff}}$ ), surface gravity ( $\log g$ ) and metallicity ( $[Fe/H]$ ), as well as rotational velocity ( $v \sin i$ ) are obtained from spectral analysis. From the estimated stellar masses, the orbital parameters of the companions are also derived. We find two types of Keplerian solutions for the companion of HD120235: (1) periods 5522 days and eccentricity of  $e \sim 0.93$ , and (2) periods 1566 days and eccentricity of  $e \sim 0.83$ . From the abundances analysis HD1695 is found to be a metal-rich star with  $[Fe/H] > 0.1$ , while HD200004 is a metal poor star with  $[Fe/H] < -0.2$ . The other two stars, HD120235 and HD145316, have solar-like abundances with  $[Fe/H] \sim 0.0$ . Our stellar parameters and orbital solutions show that all of these stars are evolved intermediate-mass giants.

© 2014 Elsevier B.V. All rights reserved.

## 1. Introduction

The thermally stabilized iodine ( $I_2$ ) gas absorption cell is one of the most powerful and widely used tool to obtain precise radial velocity (PRV) measurements of solar-type stars. In general, this absorption cell is located in front of the entrance slit of a spectrograph in order to obtain stellar and reference spectra simultaneously.  $I_2$  provides thousands of sharp spectral lines between

5000–6000 Å that are ideal for wavelength references in spectroscopy, particularly for PRV measurements. The  $I_2$ -cell is mainly used during exoplanet searches in order to detect tiny Doppler shifts of the absorption lines due to the motion of the host star around the mass center of the star-planet system (Butler et al., 1996; Sato et al., 2002). Over 1000 exoplanets have been discovered so far (see <http://exoplanet.eu>), and many of these planets have been found by using  $I_2$ -cell, based on the PRV measurement technique. In addition, the  $I_2$  cell is also used in asteroseismic studies (Frink et al., 2001) to determine low-amplitude radial velocity (RV) variations due to stellar pulsation and also to identify spectroscopic binaries.

\* Corresponding author at: Ankara University, Faculty of Science, Department of Astronomy and Space Sciences, TR-06100 Tandoğan, Ankara, Turkey. Tel.: +90 312 2126720; fax +90 312 2232395.

E-mail address: [mesutyilmaz@ankara.edu.tr](mailto:mesutyilmaz@ankara.edu.tr) (M. Yılmaz).

In 2007, we started a planet search program at TUG within the framework of an international collaboration between Turkey, Russia, and Japan. For the past seven years, we have been monitoring the RV measurements of 50 G-K type giants since such stars are suitable targets for precise measurements of Doppler shift (Frink et al., 2001; Sato et al., 2005). All the targets were selected from the HIPPARCOS catalogue (ESA, 1997) based on the following criteria: visual magnitude of  $V \sim 6.5$ , color index of  $0.6 < B - V < 1.0$ , and declination of  $\delta > -20^\circ$ . Preliminary results on the RV precision of our project have already been announced by Selam et al. (2010) and Yilmaz et al. (2013). The TUG planet search program still has been running since 2007s. During the seven years of observations we found that 9 stars show significant RV variations between 1000 and 8000  $\text{ms}^{-1}$ , while 13 targets have RV variation of 20–500  $\text{ms}^{-1}$ . The rest of targets have RV scatters of  $\sigma \sim 10 \text{ms}^{-1}$ . Our first goal is to find planets around intermediate-mass (1.3–5  $M_\odot$ ) stars in evolved stages. Such planets around intermediate-mass stars are particularly important for improving the planet formation theory, and gas giant planets around such stars provide especially important constraints on the timescale. Observational features of planetary systems over a wide range of host star masses thus need to be clarified by current and future surveys in order to understand planet formation in general. Similar searches for planets around evolved stars were carried out by Johnson et al. (2011), and recent giant planet studies includes the work of Sato et al. (2013).

The second goal of our Doppler program is also to examine nature of the other RV variations, such as spectroscopic binaries. Binary stars provide valuable information about the physical and absolute parameters of stars, such as masses and radii. The determination of absolute parameters serves us with an important knowledge about the stellar structure and evolution. Absolute orbital parameters can be obtained by analysing both the light and RV curves deduced from photometric and spectroscopic observations, respectively.

In this paper, we report the discovery of low-mass companions orbiting around the intermediate-mass giants HD1695, HD120235, HD145316 and HD200004. In addition, the stellar parameters such as effective temperature ( $T_{\text{eff}}$ ), surface gravity ( $\log g$ ), metallicity ( $[Fe/H]$ ) and rotational velocities ( $v \sin i$ ) of stars are also reported. In Section 2, we describe the observations, and in Section 3 stellar properties are presented. In Section 4, RVs and orbital solutions are given, and finally in Section 5 we discuss all the results.

## 2. Observations and data processing

We observed all the targets using CES attached to RTT150 at TUG. We used an  $I_2$  absorption cell in front of the entrance slit of the spectrograph to provide precise wavelength reference for RV measurements. The observations began in October 2007 and are still going on to monitor the target stars. In June 2009, the CCD detector was upgraded to a  $1K \times 1K$  SAO-RAS, with resolving power  $R \sim 40000$ , to  $2K \times 2K$  Andor CCD, with resolving power  $R \sim 55000$ . The CES spectra covered a wavelength region from 3500 Å to 8000 Å. We obtained signal-to-noise ratios  $S/N = 80 - 150$  per pixel with an exposure time of 1800 s for all of the targets, depending on the weather conditions. We have achieved a Doppler precision of 10–15  $\text{ms}^{-1}$  over a time span of seven years observations (Yilmaz et al., 2013).

The reduction of echelle data were performed using the IRAF<sup>1</sup> (Image Reduction and Analysis Facility) software package in the standard way (bias subtraction, normalized flat-field corrections, spectrum extraction, initial wavelength scale, etc.). Following the

**Table 1**  
Stellar parameters.

| Parameter                | HD1695           | HD120235         | HD145316         | HD200004         |
|--------------------------|------------------|------------------|------------------|------------------|
| Sp. Type                 | K0 III           | K0 III           | K0 III           | G7 III           |
| V [mag]                  | 6.54             | 6.57             | 6.61             | 6.55             |
| B-V                      | 0.99             | 0.95             | 0.95             | 0.86             |
| $\pi$ [mas]              | $5.97 \pm 0.63$  | $7.81 \pm 0.78$  | $8.21 \pm 0.97$  | $6.05 \pm 0.95$  |
| B.C.                     | -0.44            | -0.40            | -0.46            | -0.38            |
| $M_V$                    | 0.42             | 1.03             | 1.18             | 0.46             |
| $T_{\text{eff}}$ [K]     | $5000 \pm 125$   | $5075 \pm 125$   | $4950 \pm 125$   | $5125 \pm 125$   |
| $\log L_\star [L_\odot]$ | $1.87 \pm 0.09$  | $1.63 \pm 0.08$  | $1.58 \pm 0.10$  | $1.82 \pm 0.13$  |
| $\log g$ [cgs]           | $2.73 \pm 0.07$  | $2.93 \pm 0.11$  | $2.85 \pm 0.08$  | $2.84 \pm 0.13$  |
| $M_\star [M_\odot]$      | $2.6 \pm 0.32$   | $2.2 \pm 0.24$   | $1.8 \pm 0.19$   | $2.7 \pm 0.29$   |
| $R_\star [R_\odot]$      | $11.50 \pm 0.57$ | $8.47 \pm 0.42$  | $8.40 \pm 0.43$  | $10.33 \pm 0.49$ |
| $[Fe/H]$ [dex]           | $+0.14 \pm 0.08$ | $+0.06 \pm 0.11$ | $+0.02 \pm 0.14$ | $-0.22 \pm 0.07$ |
| $v \sin i$ [km/s]        | $3.4 \pm 0.53$   | $5.4 \pm 0.59$   | $3.8 \pm 0.92$   | $3.6 \pm 0.39$   |
| $\xi$ [km/s]             | $1.17 \pm 0.49$  | $1.22 \pm 0.14$  | $1.21 \pm 0.23$  | $1.40 \pm 0.13$  |
| n                        | 2                | 4                | 3                | 2                |

**Note:** n – total number of the stellar spectra.

data reduction, the spectra were normalized to the continuum level of each order by fitting a polynomial function. We used the wavelength region of 5000–6000 Å for PRV measurements where many deep and sharp  $I_2$  absorption lines exist. However, for the abundance analysis we used all echelle orders obtained without the  $I_2 - cell$ .

PRV measurements of targets were derived from the observed  $star + I_2$  spectrum using a specific IDL<sup>2</sup> code, which is based on the analysis technique described by Butler et al. (1996). In this technique, a composite  $star + I_2$  spectra are modeled as the product of a high resolution  $I_2$  and the intrinsic stellar spectrum convolved with an instrumental profile (IP) of the spectrograph. Based on this analysis technique, we divided the echelle spectrum into hundreds of spectral parts a few Å in width (typically 3.5 Å) and applied Doppler analysis to each part by comparing the model with the observations using least-square fitting. After this process, we weighted each part of the spectrum depending on the quality of model fit and value of  $S/N$ . We then derived a mean RV measurement and an error value for each exposure. Finally, we corrected this mean value to the Solar System barycenter using JPL ephemeris calculations (McCarthy, 1995). The measured velocities are not absolute radial velocities, but rather are measured relative to the iodine-free stellar template. The derived relative RVs for all the targets are listed in Tables 3–6, together with the estimated uncertainties.

## 3. Stellar parameters

In order to determine atmospheric parameters, we computed plane-parallel model atmospheres in LTE by using the ATLAS9 model grids, without the overshooting mode and with the new opacity distribution functions (Kurucz, 1993; Castelli and Kurucz, 2004). Synthetic spectra were derived using the SYNTH3 code (Kochukhov, 2007) with the help of line lists from the Vienna Atomic Line Database (VALD3; Piskunov et al., 1995; Kupka et al., 1999). We adopted Grevesse et al. (2007)'s the solar chemical composition as the reference scale during the abundances analysis. To measure the EWs of the relevant atomic lines and compare the intensity profiles of the observed and synthetic spectra, we used the BINMAG2<sup>3</sup> code, which is a graphical user interface written in IDL by Oleg Kochukhov.

We determined the effective temperature ( $T_{\text{eff}}$ ) and surface gravity ( $\log g$ ) of the stars in our sample. The effective temperatures were calculated by fitting synthetic profiles to the wings of  $H_\alpha$  and  $H_\beta$  lines, which are main temperature indicators. The surface

<sup>1</sup> <http://iraf.noao.edu>.

<sup>2</sup> <http://www.exelisvis.com/ProductsServices/IDL.aspx>.

<sup>3</sup> <http://http://www.astro.uu.se/oleg/download.html>.

**Table 2**  
Orbital parameters for all companions.

| Parameter                                     | HD1695      | HD120235   |            | HD145316   | HD200004   |
|---|-------------|------------|------------|------------|------------|
|   |             | Solution 1 | Solution 2 |            |            |
| P (days) ...                                  | 598 ±0.4    | 5522 ±251  | 1566 ±6    | 1788 ±3    | 570 ±0.6   |
| $K_1$ (kms <sup>-1</sup> ) ...                | 12.42 ±0.01 | 3.79 ±0.15 | 3.77 ±0.08 | 5.24 ±0.01 | 5.43 ±0.05 |
| e ...   | 0.17 ±0.01  | 0.93 ±0.03 | 0.83 ±0.05 | 0.14 ±0.01 | 0.01 ±0.01 |
| $\omega$ (deg) ...                            | 312 ±1      | 116 ±22    | 110 ±4     | 46 ±2      | 166 ±17    |
| $T_p$ (JD-2440000) ...                        | 4893 ±1     | 5562 ±20   | 5602 ±25   | 5597 ±6    | 5124 ±45   |
| $m_2 \sin i$ ( $M_\odot$ ) ...                | 1.17 ±0.05  | 0.21 ±0.02 | 0.21 ±0.02 | 0.52 ±0.02 | 0.45 ±0.01 |
| a (AU) ...                                    | 1.90 ±0.08  | 7.98 ±0.39 | 3.45 ±0.12 | 3.52 ±0.12 | 1.87 ±0.07 |
| $\sigma_{jitter}$ (ms <sup>-1</sup> ) ...     | 7           | 25         | 25         | 4          | 23         |
| $dv/dt$ (kms <sup>-1</sup> yr <sup>-1</sup> ) |             |            | -0.48      |            |            |
| $N_{obs}$ ...                                 | 26          | 35         | 35         | 36         | 19         |
| rms (kms <sup>-1</sup> ) ...                  | 0.018       | 0.028      | 0.030      | 0.025      | 0.027      |
| Reduced $\chi^2$ ...                          | 0.99        | 0.99       | 1.01       | 0.99       | 1.0        |

**Note:** The minimum masses of the companions  $m \sin i$  and the semimajor axes ( $a$ ) were obtained using the Table 1.

**Table 3**  
Relative radial velocities for HD1695.

| JD-2450000 | Radial velocity (kms <sup>-1</sup> ) | Uncertainty (ms <sup>-1</sup> ) |
|------------|--------------------------------------|---------------------------------|
| 5058.46817 | 0.62                                 | 18.1                            |
| 5058.48027 | 0.60                                 | 7.1                             |
| 5059.56089 | 0.47                                 | 8.8                             |
| 5080.47567 | -1.82                                | 10.3                            |
| 5080.49835 | -1.83                                | 10.5                            |
| 5474.30764 | 1.80                                 | 17.1                            |
| 5474.33019 | 1.82                                 | 18.3                            |
| 5474.35273 | 1.82                                 | 18.1                            |
| 5842.57646 | -15.13                               | 18.6                            |
| 5842.59818 | -15.13                               | 14.3                            |
| 6148.57353 | 8.54                                 | 18.4                            |
| 6148.59607 | 8.51                                 | 20.3                            |
| 6179.54482 | 7.53                                 | 18.1                            |
| 6180.53991 | 7.46                                 | 16.7                            |
| 6180.5626  | 7.44                                 | 19.8                            |
| 6200.42122 | 5.99                                 | 20.4                            |
| 6200.44375 | 6.01                                 | 19.2                            |
| 6200.46629 | 5.99                                 | 18.0                            |
| 6258.38965 | 0.11                                 | 17.5                            |
| 6258.41221 | 0.08                                 | 19.3                            |
| 6258.43477 | 0.12                                 | 18.4                            |
| 6258.45751 | 0.10                                 | 17.4                            |
| 6288.36031 | -3.10                                | 18.6                            |
| 6288.38286 | -3.14                                | 21.6                            |
| 6576.29512 | -12.41                               | 15.8                            |
| 6576.31767 | -12.43                               | 13.7                            |

**Table 4**  
Relative radial velocities for HD120235.

| JD-2450000 | Radial velocity (kms <sup>-1</sup> ) | Uncertainty (ms <sup>-1</sup> ) |
|------------|--------------------------------------|---------------------------------|
| 5001.31304 | 2.20                                 | 20.0                            |
| 5001.33575 | 2.18                                 | 6.8                             |
| 5023.28475 | 2.18                                 | 17.4                            |
| 5023.30182 | 2.19                                 | 19.2                            |
| 5265.49604 | 2.54                                 | 21.6                            |
| 5265.51785 | 2.54                                 | 20.0                            |
| 5265.53968 | 2.57                                 | 19.8                            |
| 5350.37130 | 2.75                                 | 19.4                            |
| 5350.39382 | 2.72                                 | 23.9                            |
| 5610.59448 | -3.58                                | 20.4                            |
| 5610.61705 | -3.59                                | 16.2                            |
| 5610.63963 | -3.58                                | 19.0                            |
| 6014.44466 | -0.64                                | 33.1                            |
| 6014.46720 | -0.66                                | 27.3                            |
| 6030.39901 | -0.59                                | 25.4                            |
| 6030.42154 | -0.58                                | 22.4                            |
| 6030.44409 | -0.52                                | 22.2                            |
| 6288.62713 | -0.17                                | 23.4                            |
| 6288.64968 | -0.19                                | 23.3                            |
| 6410.44478 | -0.08                                | 16.7                            |
| 6410.46733 | -0.09                                | 17.8                            |
| 6410.48988 | -0.08                                | 18.7                            |
| 6472.31498 | -0.05                                | 18.1                            |
| 6472.33754 | 0.00                                 | 15.6                            |
| 6472.36238 | 0.00                                 | 19.2                            |
| 6473.25970 | 0.01                                 | 54.9                            |
| 6473.28226 | -0.04                                | 35.1                            |
| 6668.66855 | 0.22                                 | 22.7                            |
| 6668.69113 | 0.16                                 | 17.7                            |
| 6716.44637 | 0.19                                 | 18.8                            |
| 6716.46892 | 0.2                                  | 24.2                            |

gravities were obtained from line profile fitting of gravity-sensitive lines (*MgIb* at 5167, 5172, 5183 Å, *NaI*D at 5889, 5895 Å and *CaI* at 6122, 6162 Å) and also checking the ionisation equilibrium of iron lines. For the final values of  $\log g$ , we adopted the weighted means of all derived values. The microturbulence velocities ( $\xi$ ) were determined by calculating standard deviation of both  $A(\text{FeI})^4$  and  $A(\text{FeII})$  abundances for each value of microturbulence velocity. The minimum value of the standard deviation gives the most probable value for the microturbulence velocity and the corresponding iron abundances. Rotational velocities ( $v \sin i$ ) of the stars were extracted from the unblended moderate strength spectral lines by fitting Gaussian profiles to the lines. We initially used a basic approach to estimate macro-turbulence velocities and to remove the contribution to the total line broadening. We used global macro-turbulence relationships given by Gray (1988), which is a function of parameters, such as absolute magnitude ( $M_V$ ), gravity ( $\log g$ ), and effective temperature ( $T_{\text{eff}}$ ). Luminosities ( $L/L_\odot$ ) were determined using the absolute magnitudes ( $M_V$ ) which were extracted with the help of

bolometric corrections ( $BC$ ) and parallaxes ( $\pi$ ) (ESA, 1997). The stellar radii ( $R/R_\odot$ ) were derived from  $L/L_\odot$  and  $T_{\text{eff}}$  values. Finally, stellar masses were extracted from derived stellar radii and gravity values. The stellar parameters are given in Table 1.

#### 4. Radial velocities and orbital solutions

The derived relative RVs of HD1695, HD120235, HD145316 and HD200004 are shown in Figs. 1–5 together with the best Keplerian solutions represented by the solid lines. It is clear from the figures that there are periodic variations in the RV measurements of the all systems, with an amplitude that is much larger than 2 kms<sup>-1</sup>. In order to identify any periodicity in the RV measurements, we used the generalised Lomb-Scargle periodogram (Zechmeister and Kürster, 2009; Lomb, 1976; Scargle, 1982) and sine fitting method. The periodograms of HD145316 and HD200004 show significant

<sup>4</sup>  $A(\text{FeI}) = \log[N(\text{FeI})/N(\text{H})] + 12$ .

**Table 5**  
Relative radial velocities for HD145316.

| JD-2450000 | Radial velocity (kms <sup>-1</sup> ) | Uncertainty (ms <sup>-1</sup> ) |
|------------|--------------------------------------|---------------------------------|
| 5001.40389 | 1.48                                 | 18.4                            |
| 5001.42659 | 1.48                                 | 7.2                             |
| 5024.33799 | 1.82                                 | 16.5                            |
| 5024.35402 | 1.82                                 | 16.8                            |
| 5078.25107 | 2.69                                 | 13.5                            |
| 5078.27375 | 2.70                                 | 15.6                            |
| 5290.57732 | 5.66                                 | 17.0                            |
| 5290.59994 | 5.67                                 | 18.8                            |
| 5405.29138 | 6.42                                 | 18.6                            |
| 5405.31392 | 6.43                                 | 15.6                            |
| 5405.33647 | 6.40                                 | 17.5                            |
| 5408.29630 | 6.39                                 | 41.2                            |
| 5408.31884 | 6.40                                 | 28.0                            |
| 5408.34139 | 6.39                                 | 27.0                            |
| 6021.55647 | -3.26                                | 14.9                            |
| 6021.57901 | -3.27                                | 17.4                            |
| 6021.60154 | -3.26                                | 18.2                            |
| 6080.38552 | -3.73                                | 22.3                            |
| 6080.40808 | -3.68                                | 20.9                            |
| 6080.43063 | -3.69                                | 18.5                            |
| 6149.29473 | -4.03                                | 27.7                            |
| 6149.31727 | -3.99                                | 23.2                            |
| 6353.58420 | -3.65                                | 93.1                            |
| 6353.60675 | -3.63                                | 132.2                           |
| 6407.54133 | -3.25                                | 20.7                            |
| 6407.56389 | -3.18                                | 18.4                            |
| 6407.58645 | -3.24                                | 22.2                            |
| 6469.29603 | -2.68                                | 15.9                            |
| 6469.31858 | -2.70                                | 18.2                            |
| 6469.34112 | -2.67                                | 14.5                            |
| 6525.24655 | -2.10                                | 16.6                            |
| 6525.26913 | -2.09                                | 20.4                            |
| 6526.26026 | -2.09                                | 21.0                            |
| 6526.28284 | -2.05                                | 20.6                            |
| 6707.58248 | 0.25                                 | 17.1                            |
| 6707.60502 | 0.23                                 | 18.0                            |

**Table 6**  
Relative radial velocities for HD200004.

| JD-2450000 | Radial velocity (kms <sup>-1</sup> ) | Uncertainty (ms <sup>-1</sup> ) |
|------------|--------------------------------------|---------------------------------|
| 5058.34973 | -6.38                                | 16.8                            |
| 5058.36182 | -6.38                                | 10.7                            |
| 5080.34833 | -7.41                                | 14.9                            |
| 5080.37101 | -7.40                                | 13.0                            |
| 5406.45377 | 1.86                                 | 11.9                            |
| 5406.47631 | 1.84                                 | 11.9                            |
| 5406.49885 | 1.85                                 | 12.2                            |
| 5462.37909 | 1.79                                 | 17.6                            |
| 5462.40162 | 1.76                                 | 17.9                            |
| 6084.53554 | 0.00                                 | 16.8                            |
| 6084.55828 | 0.02                                 | 19.0                            |
| 6084.58098 | 0.04                                 | 22.0                            |
| 6150.42998 | -3.70                                | 15.2                            |
| 6150.45251 | -3.69                                | 18.1                            |
| 6177.35244 | -5.19                                | 18.4                            |
| 6177.37515 | -5.21                                | 25.8                            |
| 6177.39785 | -5.23                                | 18.8                            |
| 6525.37375 | 1.42                                 | 13.6                            |
| 6525.39633 | 1.42                                 | 15.5                            |

peaks around 1786 and 570 days, respectively, with a False Alarm Probability (FAP)  $< 1 \times 10^{-6}$ . FAP of the peaks were estimated by using a bootstrap randomization method. Unfortunately, we could not find any significant period (FAP  $\leq 1 \times 10^{-1}$ ) for HD1695 and HD120235 due to the inadequate observational sampling. However, we determined a periodic cycle for these stars using a least-squares sine fitting method. The least-squares sine fitting solution for HD1695 indicates a periodic cycle around 598 days, while two different periodic cycles were derived for HD120235

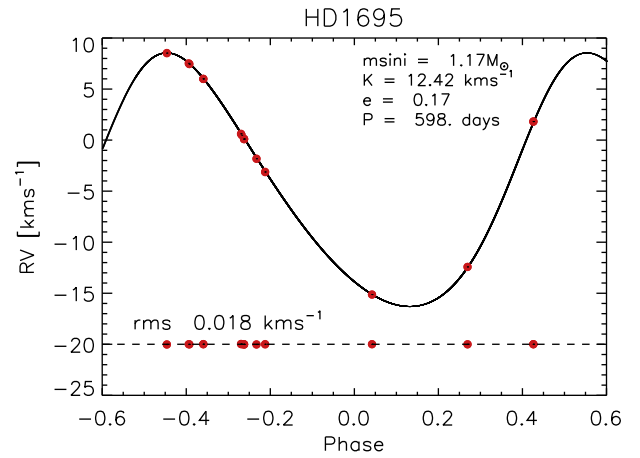


**Fig. 1.** The radial velocity curve for HD1695 and its best-fit orbital solution.

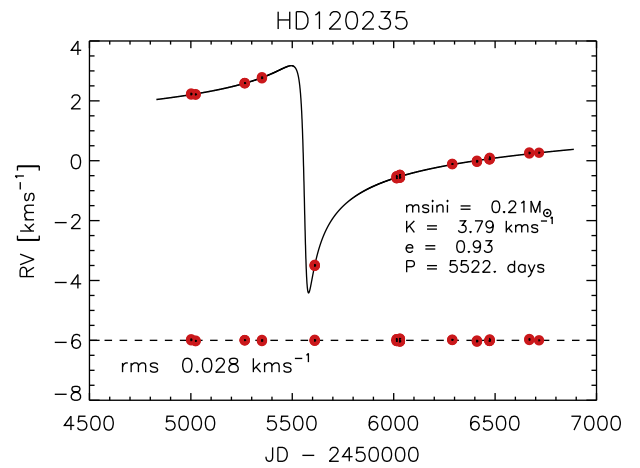


**Fig. 2.** The best-fit Keplerian model for HD120235 without removing linear trend.

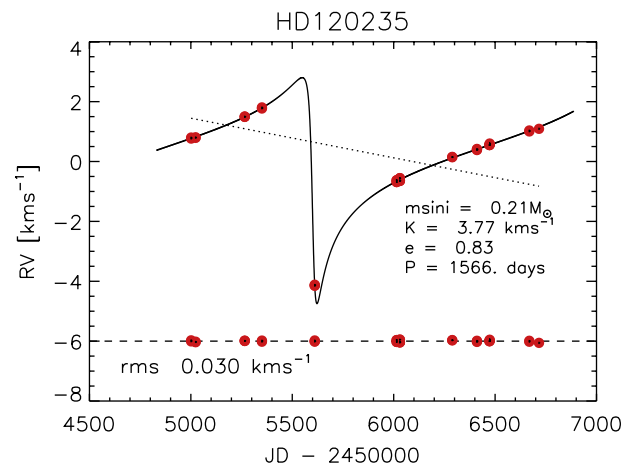


**Fig. 3.** The best-fitting orbit solution of HD120235 after removing a linear trend (dotted line). The linear trend is  $dv/dt = -0.48 \text{ kms}^{-1} \text{ yr}^{-1}$ .

with periods of 5522 and 1566 days, respectively. These two periods were obtained without removing any linear trend and applying a linear trend in the RVs of HD120235, respectively. A similar approach were also applied to the other stars, but almost the same periods were obtained. Considering the long periods for all the systems (more than several hundreds of days) and very large

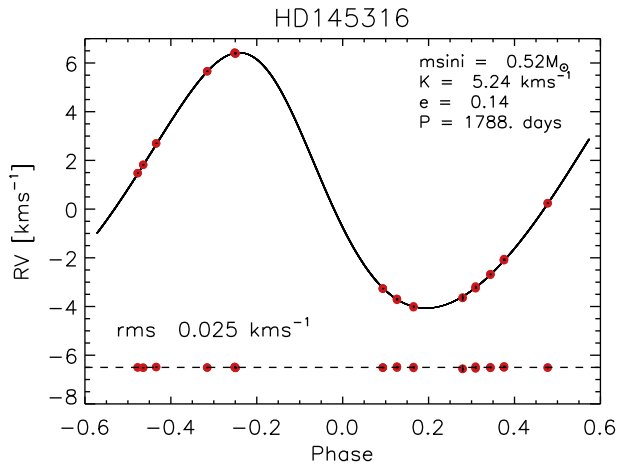


Fig. 4. The radial velocity curve of HD145316 with best orbital solution.

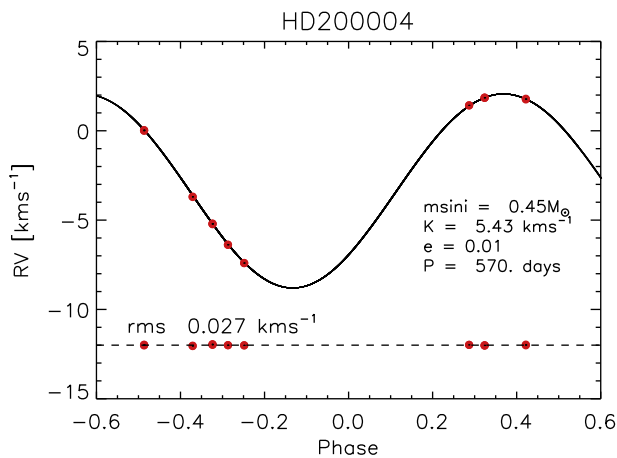


Fig. 5. The radial velocity curve of HD200004 and its best-fit orbital solution.

amplitudes (in the order of  $\text{kms}^{-1}$ ) only stellar companions may cause such high amplitudes. Furthermore, numerical simulations of G-K giants showed that the RV amplitudes are less than  $1 \text{ km s}^{-1}$  due to stellar oscillations (Hatzes et al., 1999). In addition, when we combine the stellar radii with the projected rotational velocity of the stars, we obtained rotation periods to investigate rotational modulations due to stellar spots. However, the estimated rotational periods ( $P_{\text{rot}} < 150$  days) are significantly less than the RV periods, indicating that starspots cannot be cause of such high amplitude variations in RV.

For the cases of stellar companions, the best-fit Keplerian orbits were derived using the RVLIN code, written in IDL and based on a partial linearization of the Kepler equations (Wright and Howard, 2009). All uncertainties of the orbital parameters were derived using a bootstrapping procedure. The rms of the residuals to the best Keplerian fits are about  $20\text{--}30 \text{ ms}^{-1}$ . These values are slightly larger than the typical intrinsic velocity scatters, but we assumed that these are RV jitter due to solar-like oscillations when compared with the Kjeldsen-Bedding relation (Kjeldsen and Bedding, 1995), which predicts larger amplitudes of  $20\text{--}30 \text{ ms}^{-1}$  for these stars. Therefore we determined the appropriate level of jitter empirically, by performing Keplerian fits with additional jitter ranging from zero to  $0\text{--}30 \text{ ms}^{-1}$ . All the estimated jitters were added quadratically to the RV measurements uncertainties before performing the least-squares fit of the orbits. We adopted optimal jitter values for each star when the reduced  $\chi^2$  of the fits are close to unity. Orbital solutions for all systems are given in Table 2.

Orbital solutions of HD120235 were developed in two stages. In the first stage, the RV measurements in Table 4 were solved using the period of 5522 days, which was derived without considering the linear trend in the RVs. The best Keplerian solution was obtained with an eccentricity of  $e = 0.93$ . The results are plotted as the solid curves in Fig. 2. In the second stage, the RV measurements were re-analyzed using the period of 1566 days, which was obtained after subtraction of the derived linear trend in the RVs. The RV variability was well fitted with an eccentricity of  $e = 0.83$  and a linear trend of  $-0.48 \text{ km s}^{-1} \text{ yr}^{-1}$ . The orbital solution for this stage is given in Fig. 3. A solution without the linear trend shows slightly smaller rms scatter in the residual of RVs. In both stages, orbital solutions were obtained with a highly eccentric orbit, with the second stage resulting in a slightly smaller eccentricity than the first. The minimum mass of the companion was derived in the same way for both stages.

We have performed another alternative solution for HD120235 data by considering two companion rather than one. Details of these techniques have recently been published by Wittenmyer et al. (2012a,b) and Horner et al. (2012). In this approach, we employed a genetic algorithm and run it for 100000 iterations, each consisting of 200 individual trial fits. We have achieved multiple orbital solutions in this approach that rms of residuals and reduced  $\chi^2$  are close to each other. We have not take into account these solutions for now. Follow-up observations are needed to provide clarity regarding the nature of the HD120235 system.

For all stars studied, no periodic variations indicative of substellar companions were apparent in the residual radial velocities after the effects of the stellar companion were subtracted.

## 5. Discussion and conclusions

In this study, we present PRV measurements of HD1695, HD120235, HD145316 and HD200004 for the first time. The radial velocity measurements of these stars show extremely large RV variations, and analysis indicates periodicities due to the Keplerian motion of stellar companions. There are no clear spectroscopic indications for the binarity of these stars in the literature before and there is also no evidence of astrometric motion in the HIPPARCOS data, except for HD145316, which was flagged as a binary in the study of Famaey et al. (2005) of the kinematics of K and M giants. The star HD120235 was identified as a microvariable by Koen and Eyer (2002) using HIPPARCOS (ESA, 1997) photometric data and they determined one significant frequency ( $\nu = 0.05009d^{-1}$ ) from the periodogram analysis. This period is considerably smaller than the period estimated in the present paper.

The RV measurements and stellar atmospheric parameters indicate that these stars are most likely single-lined spectroscopic binaries. The host stars for all systems are evolved intermediate-mass stars. The mass of the companions, except HD1695, are less than  $\lesssim 0.5 M_{\odot}$ . The orbital periods of the companions are greater than  $P > 500$  days and have typical low orbital eccentricities ( $0 \leq e \leq 0.3$ ), except for HD120235, which has a highly eccentric orbit. We obtained two alternative orbital solutions for HD120235. In the first solution, observed RVs was modeled without subtracting the linear trend and best fit-model was achieved with an eccentricity of  $e = 0.93$ . This eccentricity value is the largest one among all known single-lined spectroscopic binary with a giant component (De Medeiros and Udry, 1999). The orbital solution without the trend resulted in parameters consistent to within the errors of those listed in Table 2, but with larger standard deviations. In the second one, a best-fit orbital solution was obtained after subtracting the linear trend. This linear trend could

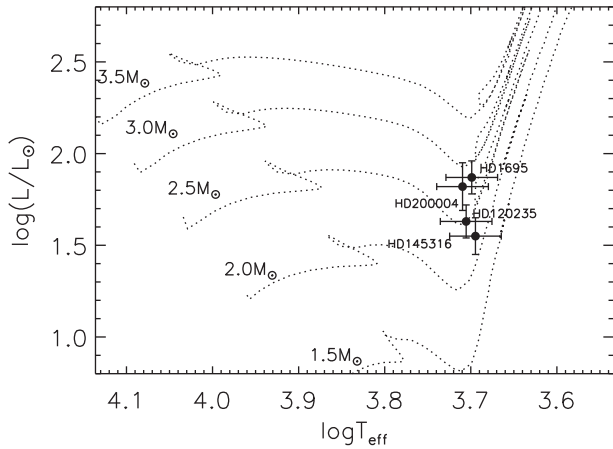


**Fig. 6.** The location of host stars in the H-R diagram with evolutionary tracks (Girardi et al., 2000) of  $Z = 0.02$  (dotted lines) for masses of  $1.5 - 3.5 M_{\odot}$ .

be explained by the presence of a second companion in a longer-period orbit, but a longer-term observations are needed.

The chemical analysis of all the targets indicate that the metallicities of HD120235 and HD145316 are close to solar abundance, while HD1695 is metal-rich, and HD200004 is a metal-poor star. From our stellar parameters, it is possible to consider the evolutionary states of all the targets in terms of the Hertzsprung–Russell (H-R) diagrams. The locations of the host stars in the H-R diagram are shown in Fig. 6. As the values of  $T_{\text{eff}}$  and  $\log g$  are relatively well determined, the largest uncertainties are in the stellar luminosity ( $L/L_{\odot}$ ) or parallax ( $\pi$ ).

### Acknowledgments

MY would like to thank The Scientific and Technological Research Council of Turkey (TÜBİTAK) for the support by BİDEB-2218 post-doctoral research scholarship. This work has been partially supported by RFBR projects 13-02-00351, 12-02-00185, 12-02-97006-r-povolzhie. Authors would like to thank TUBITAK National Observatory (TUG) and KFU for supports in using RTT150 (Russian-Turkish 1.5-m telescope in Antalya). The authors acknowledge the use of the Simbad database, operated at the CDS,

Strasbourg, France, and of NASA's Astrophysics Data System Bibliographic Services.

### References

- Butler, R.P., Marcy, G.W., Williams, E., McCarthy, C., Dossanah, P., Vogt, S.S., 1996. *PASP* 108, 500.
- Castelli, F., Kurucz, R.L., 2004. arXiv:astro-ph/0405087.
- De Medeiros, J.R., Udry, S., 1999. *A&A* 346, 532.
- ESA, 1997. The Hipparcos and Tycho Catalogues ESA SP-1200, ESA, Noordwijk.
- Famaey, B., Jorissen, A., Luri, X., Mayor, M., Udry, S., Dejonghe, H., Turon, C., 2005. *A&A* 430, 165.
- Frink, S., Mitchell, D.S., Quirrenbach, A., Fischer, D.A., Marcy, G.W., 2001. *AAS* 33, 1398.
- Girardi, L., Bressan, A., Bertelli, G., Chiosi, C., 2000. *A&AS* 141, 371.
- Gray, D.F., 1988. *Lectures on Spectral Line Analysis: F, G, and K Stars*. Aylmer, Ontario.
- Grevesse, N., Asplund, M., Sauval, A.J., 2007. *Space Sci. Rev.* 130, 105.
- Hatzes, A.P., Kanaan, A., Mkrtchian, D., 1999. *ASPC* 185, 166.
- Horner, J., Wittenmyer, R.A., Hinse, T.C., Tinney, C.G., 2012. *MNRAS* 425, 749.
- Johnson, J.A., Clanton, C., Howard, A.W., Bowler, B.P., Henry, G.W., Marcy, G.W., Crepp, J.R., Endl, M., Cochran, W.D., MacQueen, P.J., Wright, J.T., Isaacson, H., 2011. *ApJS* 197, 26.
- Kjeldsen, H., Bedding, T.R., 1995. *A&A* 293, 87.
- Kochukhov, O.P., 2007. In: Romanyuk, I.I., Kudryavtsev, D.O. (Eds.), *Proceedings of the International Conference, on the Special Astrophysical Observatory of the Russian AS, August 28–31, 2006*. *Phys. Magn. Stars*, p. 109.
- Koen, C., Eyer, L., 2002. *MNRAS* 331, 45.
- Kupka, F., Piskunov, N., Ryabchikova, T.A., Stempels, H.C., Weiss, W.W., 1999. *A&AS* 138, 119.
- Kurucz, R.L., 1993. CD-ROMs, ATLAS9 Stellar Atmospheres Programs and 2 kms<sup>-1</sup> Grid. Smithsonian Astrophysical Observatory, Cambridge, MA.
- Lomb, N.R., 1976. *Ap&SS* 39, 447.
- McCarthy, C., 1995. Master Thesis. San Francisco State University.
- Piskunov, N.E., Kupka, F., Ryabchikova, T.A., Weiss, W.W., Jeffery, C.S., 1995. *A&AS* 112, 52.
- Sato, B., Kambe, E., Takeda, Y., Izumiura, H., Ando, H., 2002. *PASJ* 54, 873.
- Sato, B., Kambe, E., Takeda, Y., Izumiura, H., Mesuda, S., Ando, H., 2005. *PASJ* 57, 97.
- Sato, B., Omiya, M., Wittenmyer, R.A., Harakawa, H., Nagasawa, M., Izumiura, H., Kambe, E., Takeda, Y., Yoshida, M., Itoh, Y., Ando, H., Kokubo, E., Ida, S., 2013. *ApJ* 762, 9.
- Scargle, J.D., 1982. *ApJ* 263, 835.
- Selam, S.O., Yilmaz, M., Izumiura, H., Bikmaev, I., Sato, B., Kambe, E., Keskin, V., 2010. In: Prsa, A., Zejda, M. (Eds.), *Binaries – Key to Comprehension of the Universe*, ASPCS, vol. 435. Astronomical Society of the Pacific, San Francisco, p. 413.
- Wittenmyer, R.A., Horner, J., Marshall, J.P., Butters, O.W., Tinney, C.G., 2012a. *MNRAS* 419, 3258.
- Wittenmyer, R.A., Horner, J., Tuomi, M., et al., 2012b. *ApJ* 753, 169.
- Wright, J.T., Howard, A.W., 2009. *ApJS* 182, 205.
- Yilmaz, M., Selam, S.O., Sato, B., Izumiura, H., Bikmaev, I., Ando, H., Kambe, E., Keskin, V., 2013. *NewA* 20, 24.
- Zechmeister, M., Kürster, M., 2009. *A&A* 496, 577.